Optical and Quantum Electronics (2024) 56:945
https://doi.org/10.1007/s11082-024-06648-5

Metamaterial-inspired MIMO antenna with negative permeability-based isolation enhancement for THz applications

Divya Saxena[1] · **Anubhav Kumar**[2]

Received: 9 October 2023 / Accepted: 12 February 2024

Abstract
A compact metamaterial-inspired two-port antenna based on negative permeability for isolation enhancement is presented. The antenna size is $65\times60\times1.5$ μm^3 where the distance to the edges of the antenna radiator is only 27 μm (0.173λ), which is less than the conventional distance (λ/2). A modified SRR-based radiator is designed using metamaterial analysis whose negative permeability is responsible for dual operating bands. Metamaterial-inspired meander-line based on negative permeability is used to increase the isolation by 31 dB at 2.1 THz. The maximum value of the isolation of the two-port antenna is 44.3 dB, which shows the low mutual coupling and surface current between the antenna elements. The MTM-inspired MIMO antenna operates at 2.1 THz and 5.3 THz. The required value of ECC and CCL of the two-port antenna is <0.05 and <0.4 bits/Sc/Hz, respectively, which shows the diversity performance and antenna can be good choice for THz operating bands.

Keywords Metamaterial (MTM) antenna · Isolation enhancement · Meander-line (ML) · THz applications · MIMO antenna

1 Introduction

Wireless communication technologies are developing rapidly with the demand for increasing bandwidth and communication rates. Nowadays, 6G communication is expected to provide larger bandwidth, higher channel capacity, and lower latency (Rajoria and Mishra 2022)

✉ Anubhav Kumar
rajput.anubhav@gmail.com

Divya Saxena
drdivyasaxena06@gmail.com

[1] Department of Applied Science & Humanities, ABES Engineering College, Ghaziabad, Uttar Pradesh 201009, India

[2] Department of Electronics and Communication Engineering, Raj Kumar Goel Institute of Technology & Management, Ghaziabad, Uttar Pradesh 201003, India

and can be used in high-rate data communication, while the terahertz (THz) frequency range from 0.1 THz to 10 THz is the potential frequency band for 6G communication (Kumar and Saxena 2020; Krozer et al. 2010). THz band has the characteristics of high resolution and high data rates with large bandwidth, but due to high path loss and molecular loss, it can be better used in areas like, imaging (Kumar and Saxena 2020; Krozer et al. 2010), biomedical, military (Yu et al. 2012), space applications (Hwu et al. 2013), short-distance communication (Kumar 2023, 2023), medicine and telecommunication (Soltanmohammadi et al. 2023). In THz wireless networks based on multiple frequency bands, multi-band antennas are better than using many single-band antennas at different frequencies. However, the metamaterial antenna is a capable and effective choice in multi-band operation with other technologies such as defected ground, fractal, and slot antenna. Metamaterials also play an important role in designing the effective absorber (Meng 2022; Lan et al. 2021; Ruan et al. 2022a, b, 2023) and filter (Ruan et al. 2021) for THz applications. Metamaterial-inspired radiators can miniaturize the antenna (Ruan et al. 2022a, b; Wen et al. 2018) and provide resonant modes depending on the application, where most natural materials have weak electrical and magnetic responses, while metamaterials may be more effective at controlling radiation (Withayachumnankul 2009). However, the application of THz signals in wireless communications cannot be effectively performed with a single-element antenna, whereas this problem can be easily solved in a MIMO antenna. MIMO antennas can be compact by reducing the distance between antenna elements, but this increases mutual coupling, which has a detrimental effect on antenna performance because mutual coupling is inversely proportional to the distance between antennas. Although mutual coupling can be traditionally reduced by increasing the distance between antennas, this also increases the size of the MIMO antenna. In the literature, several MIMO antennas have been discussed without decoupling networks for THz frequency application, using unconnected ground (Babu et al. 2022; Keshwala 2021; Vasu Babu et al. 2022) and distance of the antenna elements (Das and Nahar 2022) is greater than or equal to a quarter wavelength whereas with decoupling network such as the defective ground/stub (Kumar 2023; Das and Nahar 2022; Prabhu and Malarvizhi 2022; Saxena et al. 2022), Graphene (Kumar et al. 2023), MTM absorber (Saxena et al. 2022), and slots (Singh and Varshney 2023). Complex decoupling and distances between antennas which increase the size of the antenna size may not be a good practice for practical applications. In (Kumar 2023), Two-microstrip-fed radiators are placed orthogonally to achieve polarization diversity with the defected ground where the SRR-based graphene is used to diminish the coupling current. In (Kumar et al. 2023), Two-half-cut inspired radiators are used where the T-stub and asymmetric slot perfectly weak the coupling. In (Babu et al. 2022), the fractal shape patch is used on the polyimide material with 82.37% efficiency with unconnected ground. In (Keshwala 2021), a rectangular patch is modified to a sinusoidal patch to expand the bandwidth with the unconnected ground. In (Vasu Babu et al. 2022), a tree-shaped radiator is used for bandwidth improvement with an unconnected ground two-port antenna with low radiation efficiency. In (Das and Nahar 2022), a circular-shaped radiator is modified, and defective ground changes in the lumped element are used to improve the IM and bandwidth. The distance between elements is half wavelength, which helps to provide high isolation. In (Prabhu and Malarvizhi 2022), a Koch fractal-shaped radiator is used with the defective ground on a polyimide substrate where the F-shaped stub with the circular slot is used to moderate the surface wave. In (Saxena et al. 2022), slot-loaded rectangular-shaped radiator with CSRR loaded in the ground is used in

the THz MIMO antenna with Quart material where the MTM absorber is used to diminish the coupling for isolation. In (Singh and Varshney 2023), the shared rectangular radiator is used with silicon dioxide where the multiple slots in the single radiator perturb the current flow for improvement in the isolation. The graphene material is loaded on the antenna for tuning the isolation. In (Varshney et al. 2019), microstrip-fed as a patch is situated in the front with a graphene patch that is loaded on the radiator. After literature analysis, an MTM-inspired MIMO antenna for dual-band THz application and negative permeability-based decoupling are used to reduce the size of the antenna where simple decoupling can be an effective choice for practical applications. In this design, silicon-based substrate is used due to its application in biomedical as well as effective compatibility with electronic devices (Dash 2021; Bhuyan et al. 2014). The technology and technical implications of the proposed antenna are highlighted below.

1. The antenna is arranged on the silicon dioxide material which shows the effective radiation efficiency for THz applications.
2. The radiator is based on the MTM characteristics where the negative value of the permeability is responsible for the dual operating bands.
3. The proposed MTM-inspired two-port antenna is compact in design which is possible with a meander line based on the negative value of the permeability. The meander-line in the ground successfully reduces and perturbs the ground current from port-1 to port-2.
4. The meander-line in the ground without complex decoupling, effectively diminishes the ground current and increases the isolation to 31 dB where the gap between radiating elements is 0.173λ.

2 Design of the antenna

The implementation of an MTM-inspired antenna for THz application is complex due to the small antenna size therefore silicon-dioxide material with simple and effective decoupling is used to demonstrate for design of the MIMO antenna with εr=3.9 and tan (δ)=0.0006 (Kumar 2023). THz systems have a lot of complexity in fabrication (Kumar et al. 2023) while MIMO antennas can be fabricated by CNC (Ashvanth and Partibane 2021) and micromachining (Ermolov et al. 2018; Huang and Kuo-Yi 2012) methods although micromachining methods may be more effective. Gold as a conducting material is used with a thickness of 35 nm and the size of the MTM-inspired antenna is only 65×60×1.5 μm^3. The antenna dimension parameters are as follows (in μm) as represented in Fig. 1(a): Lu=20, Wu=20, Lu1=2, Lu2=10, Lu3=11, Lu4=2, Lu5=8, Lu6=10, Lu7=8, Lu8=9, L=60, Wf=3, L5=2, L2=22, L4=8, L3=26, W=65, L1=29, L6=5.5, L8=9, L7=6. The development steps are based on the three steps and are explained in Fig. 1 (b-f) as steps 1 to 5 with their S-parameters.

When $\frac{W_f}{t} > 1$ then

$$Z_0\,(\text{Characteristics}\,i\text{mpedance}) = \frac{120\pi}{\sqrt{\epsilon_{eff}}\left[\frac{W_f}{t} + 1.393 + \frac{2}{3}\ln(\frac{W_f}{t} + 1.444)\right]} \quad (1)$$

Where

$$\epsilon_{eff}\,(\text{effective dielectric constant}) = \frac{\epsilon_{r+1}}{2} + \frac{(\epsilon_r - 1)}{2}\left[1 + 12\frac{t}{w_f}\right]^{-\frac{1}{2}} \tag{2}$$

In the first step, a circular-shaped radiator is used with a microstrip-fed transmission line and partial ground which increases the Impedance Matching (IM) and provides the Impedance Bandwidth (IBW). The width of the microstrip line is calculated from Eq. 1 where the characteristics impedance (Zo) is 50 ohm. The partial ground length is 22 μm and the width is 19.5 μm which is responsible for impedance matching of the single band. The operating bandwidth of the two-port antenna is 19.5 THz to 2.4 THz where the unconnected ground is used in the two-port antenna and achieved isolation is higher than 10 dB. In the second step, the circular-shaped radiator converts into the split ring resonator-shaped radiator which is responsible for the dual operating band. The operating bandwidth of the two-port antenna is 1.9 THz to 2.35 THz and 5.4 to 6.05 THz with more than 20 dB isolation in a higher frequency band and more than 10 dB isolation in the lower frequency band. In the third step, the SRR-shaped radiator is modified which shifts the higher frequency band towards to lower frequency. The MTM characteristics of the modified SRR-shaped radiator are analyzed and found the negative permeability. The obtained bandwidth slightly changes as compared to the MTM characteristics due to the optimized value of partial ground. The distance of the antenna in a two-port design is less than a quarter wavelength which increases the surface current and reduces the isolation. The IBW of this step obtains from 1.85 THz to 2.25 THz and 4.9 THz to 5.6 THz. The isolation in the lower band is from 10.7 dB to 12 dB and 19 dB to 28 dB in the higher band. In the fourth step, the ground plane is connected to the antenna and creates the common ground plane for practical application. The common ground improves the length of the ground plane and improves the IBW of the lower band. The IBW of this step obtains from 1.8 THz to 2.4 THz and 4.75 THz to 5.5 THz where the antenna exhibits a strong surface current and low isolation. The isolation in the lower band is from 9 dB to 19 dB and 19 dB to 22.5 dB in the higher band. In the fifth step, a metallic strip-based meander line is implanted in the ground which results tremendously and controls the surface wave as well as perturbs the wave in the different direction between ports. The MTM characteristics of the meander-line are determined which shows the negative permeability at 2 THz and is responsible for isolation improvements. The current variation in the magnitude and vector representation at 2.1 THz and 5.3 THz are characterized in Fig. 1 (g-h) and (i-j) where the effectiveness of the meander-line is visible which diminishes and controls the surface current. The vector representation in the meander line is different direction which controls the flow of the current and reduces the coupling effect. The MIMO antenna operates at 2.1 THz and 5.3 THz with operating bandwidth from 1.93 THz to 2.35 THz and 4.95 THz to 5.6 THz where the antenna exhibits a low coupling current and high isolation. The isolation in the lower band is from 20.2 dB to 44.3 dB and 20.1 dB to 32.3 dB in the higher band. The meander-line effectively diminishes the ground current and increases the isolation up to 31 dB when the edge-to-edge distance of antenna elements is only 0.173λ.

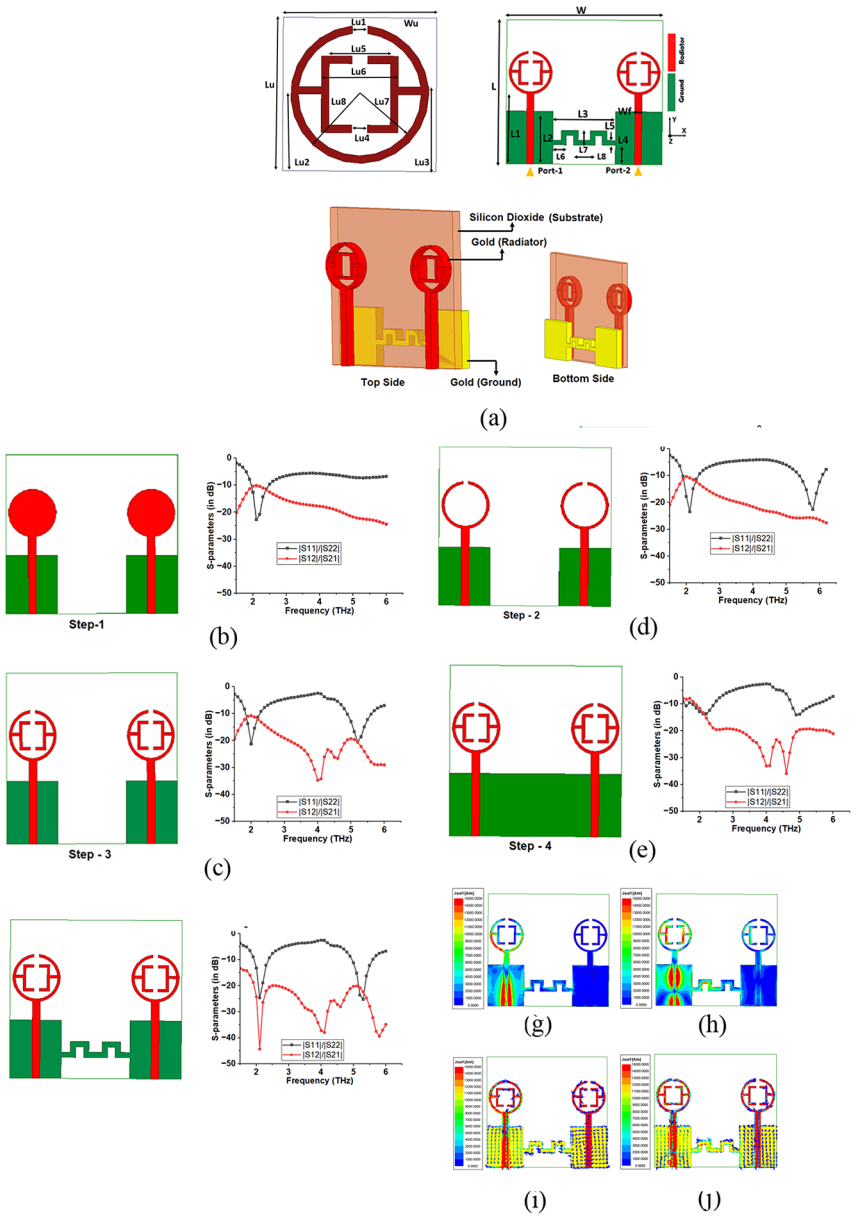

Fig. 1 THz MIMO antenna (**a**) Design of the two port Antenna with 3D view (**b**) – (**f**) Evolution steps with |S11| and |S12|, current analysis at 2.1 THz and 5.3 THz in magnitude (**g-h**) and in vector (**i-j**)

3 Metamaterial analysis

The metamaterial (MTM) characteristics of the radiator and meander-line decoupling are used to determine the reflection (|S11|) and transmission coefficient (|S12|) as characterized in Fig. 2 (a) and (b). The s-parameters of the MTM radiator are extracted as shown

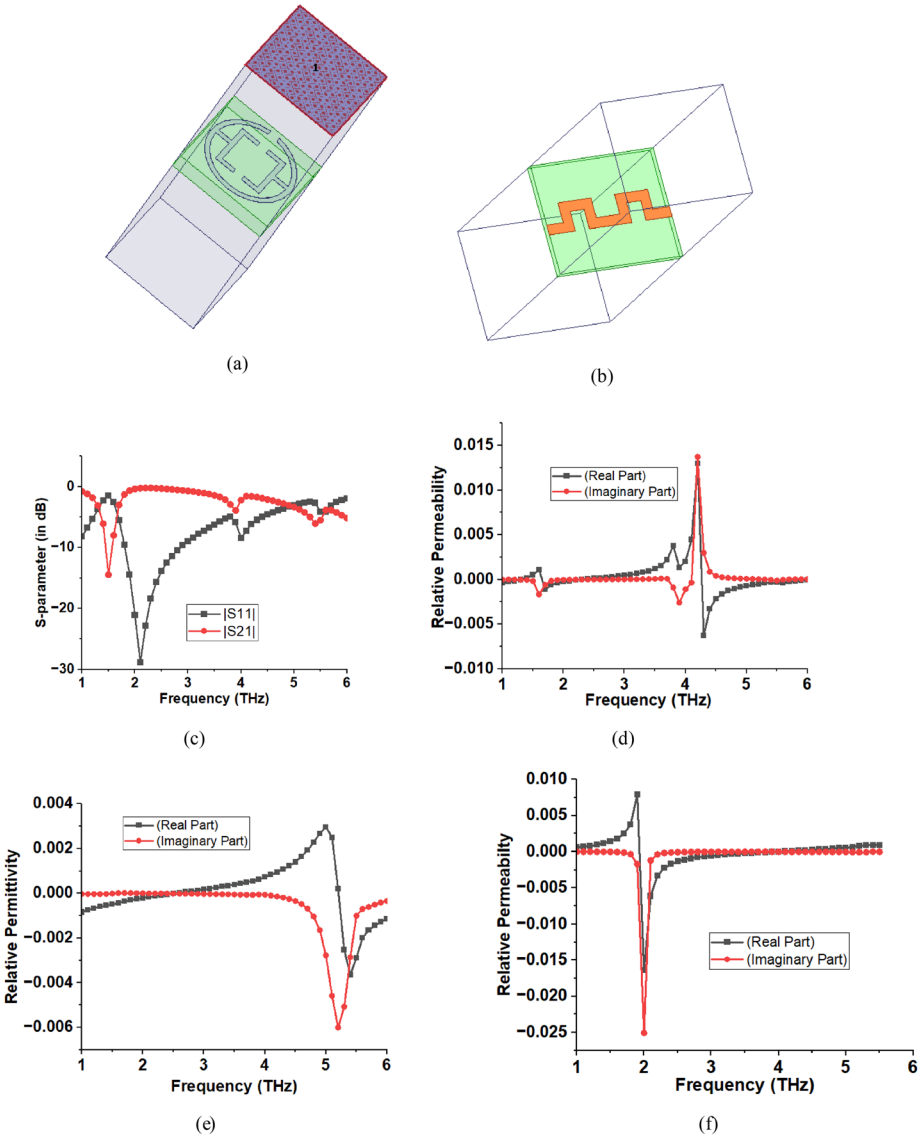

Fig. 2 Metamaterial Analysis of antenna radiator (**a**) Simulation set-up of radiator (**b**) Simulation set-up of Meander-line (**c**) s-parameters of radiator (**d**) Extracted relative permeability of radiator (**e**) Extracted relative permittivity of radiator (**f**) Extracted relative permeability of meander-line

in Fig. 2 (c) by the boundary conditions in the x and y direction applied perfect magnetic and electric conductors (PMC and PEC) where wave port in the top and bottom plane as represented in Fig. 2 (a). The red curve represents the stop-band and the black curve represents the pass-band characteristics. The extracted MTM characteristics are determined by the Nicolson Ross-Wier (NRW) (Ziolkowski 2003) Eq. 3 to 6 from s-parameters. Figure 2 (d and e) shows the extracted relative permeability and relative permittivity of the antenna

radiator. The real resonant value of negative relative permeability is found at 1.7 THz and 4.3 THz. The real resonant value of negative relative permittivity is found on 5.4 THz. The negative permeability affects and is responsible for the operating band of the antenna where the MTM-inspired two-port antenna operates at 2.1 THz and 5.3 THz. Some variation in MTM characteristics and achieved antenna bandwidth is observed due to ground plane and feed length optimization for impedance matching. The analysis of the meander-line as represented in Fig. 2(b), is revealed in Fig. 2(f), where extracted relative permeability is negative at 2 THz and performs a strong barrier for current in the antenna. The negative relative permeability is responsible for isolation enhancement up to 31 dB at 2.1 GHz when the distance of the radiators is only 0.173λ.

$$V_1 = S_{11} + S_{21} \tag{3}$$

$$V_2 = S_{21} - S_{11} \tag{4}$$

Where Ko is defined as the wave vector and t is defined as a thickness of the material and

$$\mu_{\mathrm{r}} \sim \frac{(1 - V_2)}{(1 + V_2)} \frac{2}{\mathrm{j}\mathrm{k}_0\mathrm{t}} \tag{5}$$

$$\varepsilon_{\mathrm{r}} \sim \frac{(1 - V_1)}{(1 + V_1)} \frac{2}{\mathrm{j}\mathrm{k}_0\mathrm{t}} \tag{6}$$

4 EC-model investigation

The MTM-inspired antenna is designed for dual-band operating bandwidth where the meander line is used to perturb the coupling current. The electronic circuit (EC) model based on RLC lumped components is used to validate the s-parameters as illustrated in Fig. 3 (a). The Lf1/Lf2 and Cf1/Cf2 are used to represent the microstrip fed, two RLC tank circuit Cp1/Cp2, Lp1/Lp2, Rp1/Rp2 and Cr1/cr2, Lr1/Lr2, Rr1/Rr2 are used to represent the dual operating bands and Ld, Rd, Cd is used to represent the meander line decoupling technology. The circuit is designed using the Quite Universal Circuit Simulator (QUCS) circuit simulator where RLC components are determined with the tuning phenomena (Kumar et al. 2023). The s-parameters are determined with HFSS and QUCS software as represented in Fig. 3 (b) where the |S11| response is approximately similar and |S21| parameters are more than 20 dB which validates the results.

5 Results and discussion

The proposed antenna is established with an MTM-inspired radiator and negative permeability-based meander-line in the ground which is designed on an HFSS-19 simulator. The silicon dioxide material is used the design the antenna for THz frequency to investigate the MIMO antenna. The MIMO antenna operates at 2.1 THz and 5.3 THz with operating

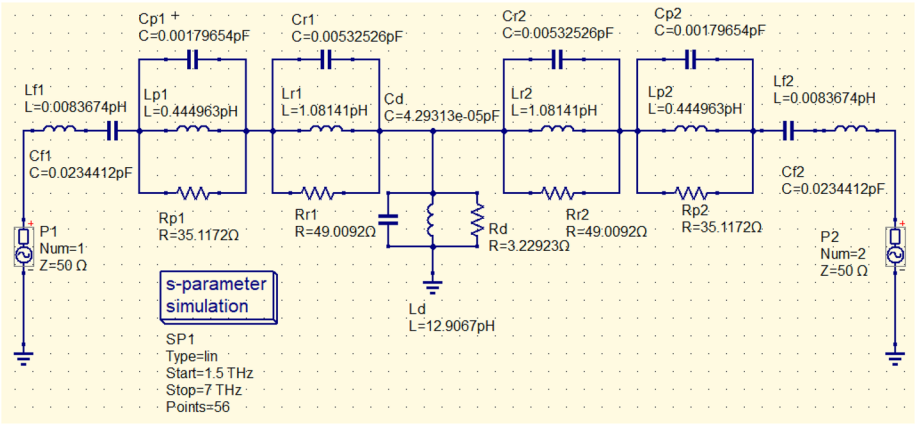

(a)

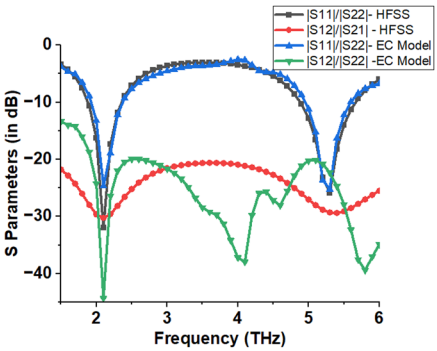

(b)

Fig. 3 EC Model (**a**) EC model on QUCS (**b**) S-parameters from EC model and HFSS

bandwidth from 1.93 THz to 2.35 THz and 4.95 THz to 5.6 THz as described in Fig. 4 (a). The isolation response is based on the meander-line and negative permeability, which weakens the coupling produces the discontinuity in the ground, and increases the port isolation greater than 31 dB. The efficiency and gain are represented in Fig. 4 (b) and (c) where the efficiency represents the accepted power and radiated power which shows the effect of the material and the effectiveness of the design at the THz frequency. The efficiency is found to the more than 65% and the maximum value is 79.3%. The gain of the lower band is 1.1 to 1.6 dB and 2.2 to 2.6 at the higher band where the highest value is 2.6 dB. The far-field pattern in normalized value is represented in the different planes as discussed in Fig. 4 (d), which shows the omnidirectional and stable response. The two-port antenna can be used in small-distance communication, imaging and biomedical THz frequency applications. The MIMO parameters are investigated to determine the diversity performance of the antenna, therefore, Envelope Correlation Coefficient (EC-C), Diversity Gain (D-G), total active reflection coefficient (TAR-C), and Channel Capacity Loss (C-CL) factors are determined from the simulated s-parameters from Eq. 7 to 11 as demonstrated in Fig. 4 (e-h). The ECC represents the antenna elements that received signal affected by the other antenna elements

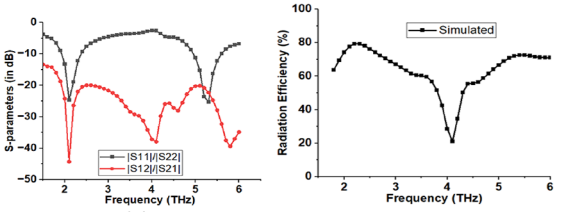

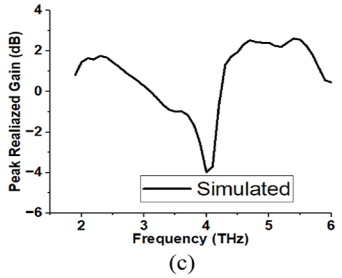

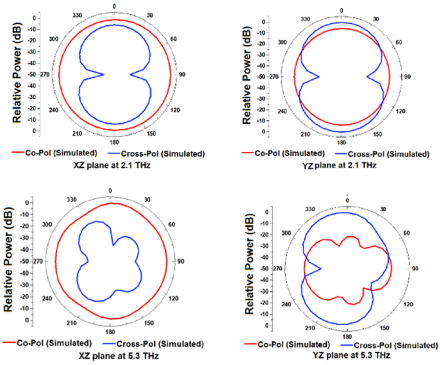

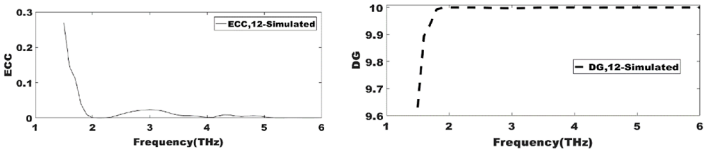

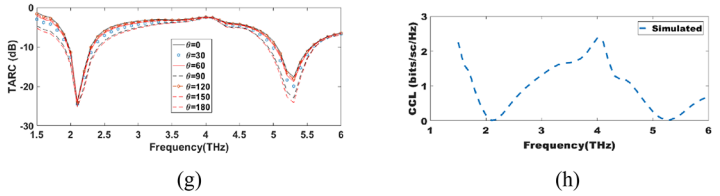

Fig. 4 Investigation results (**a**) S-parameters (**b**) Efficiency (**c**) Gain (**d**) Far-field pattern (**e**) EC-C (**f**) D-G (**g**) TAR-C (**h**) CC-L

and output independency of the antenna elements from the other antenna elements. When one antenna element radiates without affecting the other antenna elements its value should be zero but in practical applications considered less than 0.5. The ECC value is less than 0.05 in the proposed antenna which represented the low coupling and less power affected from one element to other elements. The signal-to-interference ratio from multiple to the single antenna where higher value represents the low coupling by the DG. The proposed antenna has approximately 10 dB which represents good diversity performance.

$$\boldsymbol{ECC} = \frac{\left|\boldsymbol{S}_{11}^{*}\boldsymbol{S}_{12} + \boldsymbol{S}_{21}^{*}\boldsymbol{S}_{22}\right|^{2}}{\left(1 - \left|\boldsymbol{S}_{11}\right|^{2} - \left|\boldsymbol{S}_{21}\right|^{2}\right)\left(1 - \left|\boldsymbol{S}_{22}\right|^{2} - \left|\boldsymbol{S}_{12}\right|^{2}\right)} \tag{7}$$

$$\boldsymbol{DG} = 10\sqrt{1 - \left|\boldsymbol{ECC}\right|^{2}} \tag{8}$$

$$TARC = \frac{\sqrt{\sum_{i=1}^{N}\left|b_i\right|^{2}}}{\sqrt{\sum_{i=1}^{N}\left|a_i\right|^{2}}} \tag{9}$$

$$\boldsymbol{TARC} = \frac{\sqrt{\left(\left|\boldsymbol{S}_{11} + \boldsymbol{S}_{12}\boldsymbol{e}^{\boldsymbol{j\theta}}\right|^{2} + \left|\boldsymbol{S}_{22}\boldsymbol{e}^{\boldsymbol{j\theta}} + \boldsymbol{S}_{21}\right|^{2}\right)}}{\sqrt{2}} \tag{10}$$

$$\boldsymbol{CCL} = -\boldsymbol{log}_{2}\boldsymbol{det}\left(\boldsymbol{\psi}^{\boldsymbol{R}}\right) \tag{11}$$

The TARC is characterized by the ratio of the returned power to the applied power in the square root as illustrated in the Eq. 10 and considered the s-parameters from Eq. 11 which demonstrated the antenna bandwidth. The TARC has minimum deviation at the different phase angles from the other antenna elements of the two-port antenna. The CCL refers to the data transfer rate of the MIMO antenna where the accepted value is 0.04 bits/sec/Hz and is limited to under-limit and validate the diversity performance. The comparative investigation in terms of size, decoupling network, and isolation is illustrated in the Table 1. In, (Babu et al. 2022), (Keshwala 2021), and (Vasu Babu et al. 2022) used distance and unconnected ground to improve the isolation where the (Keshwala 2021), (Vasu Babu et al. 2022) and (Das and Nahar 2022) not reported the efficiency. In, (Prabhu and Malarvizhi 2022), (Saxena et al. 2022), (Singh and Varshney 2023), and (Kumar et al. 2023) have used large sizes of antenna. The proposed MIMO antenna is designed as a compact antenna compared to the existing antenna with high isolation and simple decoupling which makes it easy to fabricate in THz applications.

Table 1 Comparative description of MIMO antenna for THz applications

Reference (Years)	Material used	Antenna size(μm x μm)	|S11|/|S22| dB (THz)	|S12|/|S21| (dB)	Antenna /Decoupling Network
(Kumar 2023)	Silicon dioxide	30×30	4.9 to 6.3	>24.8	Graphene SRR
(Kumar et al. 2023)	Polyimide	100×105	1.74 to 2.52	>20	Defected Ground
(Keshwala 2021)	Polyimide	100×180	1.01 to 2.21, 5.64 to 37.5	20	Sinusoidal patch/ separated ground
(Vasu Babu et al. 2022)	Polyimide	600×300	0.276–0.711	>20	Tree-shaped radiator / unconnected ground
(Das and Nahar 2022)	polyamide	1219×800	0.12–11.964	>25	Modified circular radiator/Defected ground
(Prabhu and Malarvizhi 2022)	polyimide	1400×750	0.3 and 10	>20	Koch fractal/F-shaped stubs
(Saxena et al. 2022)	Quart	480×480	0.52–1.47	>20	Butterfly-shaped ground/MTM absorber
(Singh and Varshney 2023)	silicon dioxide	100×150	4.93 and 5.43	>18.65	Shared rectangular radiator/Slots
(Varshney et al. 2019)	silicon dioxide	60×40	1.76 – 1.87	25	Microstrip-fed/ graphene Patch
Proposed	Silicon dioxide	65×60	1.93 to 2.35 and 4.95 to 5.6	>20	MTM radiator and MTM decoupling

6 Conclusion

The MTM-inspired MIMO antenna with dual operating bands is designed for THz operation. The negative permeability of the radiator and meander line decoupling are responsible for the dual-band operation and low mutual coupling. The meander line in the ground plane weakens the coupling and increases the isolation up to 31 dB when the gap of antenna edges is only 0.173λ. The simple decoupling technique is useful for THz applications where this type of decoupling structure simplifies antenna fabrication. The MIMO antenna operates at 2.1 THz and 5.3 THz with more than 20 dB isolation. The proposed dual-band two-port antenna with good diversity characteristics can effectively work for THz applications.

Author contributions Anubhav Kumar design the Two-port antenna and validation of the results, Divya saxena completed the mathematical analysis of metamaterial radiator and Meander-line decoupling network as well as design the EC Model. Both authors wrote and reviewed the manuscript.

Funding Not applicable.

Data availability Not applicable.

Code availability Not applicable.

Declarations

Competing interests The authors declare no competing interests.

References

Ashvanth, B., Partibane, B.: Multiband characterized high gain MIMO antenna for terahertz applications. Opt. Quant. Electron. **53**, 460 (2021)

Babu, K., Vasu, et al.: Design and optimization of micro-sized wideband fractal MIMO antenna based on characteristic analysis of graphene for terahertz applications. Opt. Quant. Electron. **54**, 281 (2022)

Bhuyan, M.K., et al.: Silicon substrate as a novel cell culture device for myoblast cells. J. Biomed. Sci. **21**, 1–5 (2014)

Das, V., Nahar, T.: Design and analysis of sectored-circular planar antenna with defected ground for WBAN and MIMO applications. Opt. Quant. Electron. **54**(11), 752 (2022)

Dash, S.: Impact of silicon-based substrates on graphene THz antenna. Phys. E: Low-dimensional Syst. Nanostruct. **126**, 114479 (2021)

Ermolov, V., et al.: Micromachining integration platform for sub-terahertz and terahertz systems. Int. J. Microw. Wirel. Technol. **10**, 5–6 (2018)

Huang, I.-Y., Chian-Hao Sun, and, Kuo-Yi, H.: Improving bandwidth and return loss of Si-based MEMS antenna using suspending and electromagnetic band-gap structures. Sens. Actuators A: Phys. **174**, 33–42 (2012)

Hwu, S.U., Kanishka, B., deSilva, Cindy, T., Jih: Terahertz (THz) wireless systems for space applications. In *2013 IEEE Sensors Applications Symposium Proceedings*, pp. 171–175. IEEE, (2013)

Keshwala, U.: Microstrip line fed sinusoidal tapered square shaped MIMO antenna for THz applications. Optik. **247**, 167905 (2021)

Krozer, V., et al.: Terahertz imaging systems with aperture synthesis techniques. IEEE Trans. Microwave Theory Tech. **587**, 2027–2039 (2010)

Kumar, A.: Graphene based SRR with quadrupole mode loaded on two port antenna with high isolation and polarization diversity for THz applications. Opt. Quant. Electron. **55**, 1043 (2023)

Kumar, A., Saxena, D.: Compact UWB Microstrip Antenna for THz Communication Application. In *9th International Conference System Modeling and Advancement in Research Trends (SMART)*, pp. 388–391. IEEE, (2020)

Kumar, A., et al.: Compact two-port antenna with high isolation based on the defected ground for THz communication. Results Opt. **13**, 100522 (2023)

Lan, F., et al.: All-dielectric water-based metamaterial absorber in terahertz domain. Opt. Mater. **121**, 111572 (2021)

Meng, Z.: Broadband-absorption mechanism in a water-based metamaterial absorber. Phys. Lett. A. **445**, 128269 (2022)

Prabhu, P., Malarvizhi, S.: Koch fractal loaded high gain super-wideband diversity THz MIMO antenna for vehicular communication. Opt. Quant. Electron. **54**(11), 726 (2022)

Rajoria, S., Mishra, K.: A brief survey on 6G communications. Wireless Netw. **28**(7), 2901–2911 (2022)

Ruan, J., et al.: Ultra-wideband THz metamaterial filter with steep cut-off. J. Electromagn. Waves Appl. **35**(4), 431–440 (2021)

Ruan, J., Fu, et al.: Surface plasmon resonance-enhanced broadband perfect absorption in a Ti3C2Tx-based metamaterial absorber. J. Phys. D. **55**, 485102 (2022a)

Ruan, J.-F., et al.: Tunable terahertz metamaterial filter based on applying distributed load. Phys. Lett. A. **421**, 127705 (2022b)

Ruan, J., Fu, et al.: Perfect absorption based on Ti3C2Tx surface plasmon resonance. Opt. Mater. **137**, 113604 (2023)

Saxena, G., et al.: Metasurface inspired wideband high isolation THz MIMO antenna for nano communication including 6G applications and liquid sensors. Nano Commun. Netw. **34**, 100421 (2022)

Singh, R., Varshney, G.: Isolation enhancement technique in a dual-band THz MIMO antenna with single radiator. Opt. Quant. Electron. **55**(6), 539 (2023)

Soltanmohammadi, H., Jarchi, S., Soltanmohammadi, A.: Tunable dielectric resonator antenna with circular polarization and wide bandwidth for terahertz applications. Optik **287**, 171124 (2023)

Varshney, G., Gotra, S., Pandey, V.S., Yaduvanshi, R.S.: Proximity-coupled two-port multi-input-multi-output graphene antenna with pattern diversity for THz applications. Nano Commun. Netw. **21**, 100246 (2019)

Vasu Babu, K., et al.: A micro-scaled graphene-based tree-shaped wideband printed MIMO antenna for terahertz applications. J. Comput. Electron. **21**(1), 289–303 (2022)

Wen, D., et al.: Geometric metasurfaces for ultrathin optical devices. Adv. Opt. Mater. **6**, 1800348 (2018)

Withayachumnankul, W.: Metamaterials in the terahertz regime. IEEE Photonics J. **1**(2), 99–118 (2009)

Yu, C., et al.: The potential of terahertz imaging for cancer diagnosis: A review of investigations to date. Quant. Imaging Med. Surg. **21**, 33 (2012)

Ziolkowski, R.W.: Design, fabrication, and testing of double negative metamaterials. IEEE Trans. Antennas Propag. **51**(7), 1516–1529 (2003)